

Sol-Gel Synthesis of Manganese Oxides

S. BACH,¹ M. HENRY, N. BAFFIER, AND J. LIVAGE

Laboratoire de Chimie de la Matière Condensée, Ecole Nationale Supérieure de Chimie de Paris, 11 rue Pierre et Marie Curie, 75231 Paris Cedex 05, France

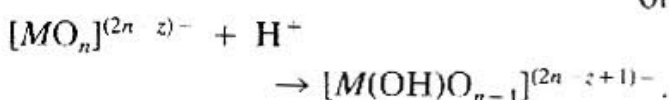
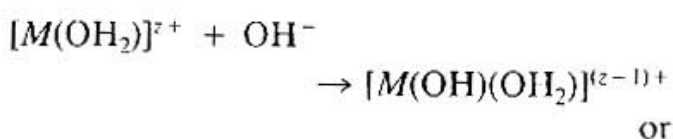
Received March 14, 1990; in revised form May 14, 1990

Transparent and stable manganese dioxide gels are obtained upon reduction of permanganate aqueous solutions $AMnO_4$ [$A = Li, Na, K, NH_4, N(CH_3)_4$] by fumaric acid. All xerogels are amorphous when dried at room temperature. Their thermal behavior however depends on the nature of the counter cation A^+ . Ammonium permanganates lead to the formation of α - or γ - Mn_2O_3 while $AMnO_2$ mixed oxides are obtained at high temperature when $A = Li, Na, K$. Other crystalline phases such as $LiMn_2O_4$ or $Na_{0.7}MnO_2$ are also formed at lower temperature around 500°C. Oxidation of these mixed oxides into sulfuric acid lead to the formation of λ - or δ - MnO_2 while A^+ and Mn^{2+} ions are released into the solution. Such manganese dioxides could be good candidates for making reversible cathodes in nonaqueous lithium batteries. © 1990 Academic Press, Inc.

Introduction

Manganese oxides such as manganese dioxide MnO_2 are very attractive materials as reversible cathodes in nonaqueous lithium batteries (1-4). One of the main advantages of MnO_2 is its high discharge voltage. Reversible cathodes are generally made with crystalline oxides. Their electrochemical properties however strongly depend on parameters such as powder morphology, crystalline structure, or bulk density. The sol-gel process, based on inorganic polymerization reactions from molecular precursors (5), offers an alternative route to the synthesis of oxide powders. It allows a better control of the morphology and texture of solid particles (6, 7). Sol-gel chemistry in aqueous solutions is based on hydrolysis

and condensation of metal ions. Hydroxylation is usually performed via pH modification either by adding a base to a low valent hydrated cation or an acid to a high valent oxo anion as follows:



Condensation then follows via olation or oxolation leading to the formation of an oxide or hydroxide network. One of the main problems for the sol-gel synthesis of MnO_2 is the lack of stable Mn(IV) precursors in aqueous solution. This can be overcome by performing hydroxylation via redox reactions rather than acid-base reactions. The precursor is then a soluble manganese salt in which the oxidation state of Mn is different

¹ To whom correspondence should be addressed.

from four. The *in situ* formation of Mn(IV) solute species is then obtained via oxidation or reduction reactions. One of the most common methods is to mix an inorganic precursor such as KMnO_4 with reducing agents in an alkaline or acidic medium (5). However, such reactions are usually performed with rather dilute solutions so that colloidal solutions are obtained rather than gels.

This paper reports on the synthesis of monolithic manganese oxide gels through the reduction of AMnO_4 ($A = \text{Li, Na, K, NH}_4, \text{N(CH}_3)_4$) aqueous solutions. The chemical composition and the crystalline structure of the resulting product depend on many parameters such as the pH of the solution, the chemical nature of the reducing agent, and even the counter cation A . Only the role of this last parameter will be discussed here.

Experimental

Gel formation from aqueous permanganate solutions depends on the chemical nature of the organic reducing agent. The best results were obtained with fumaric acid ($\text{C}_4\text{H}_4\text{O}_4$). Gels are rapidly formed (20–30 min) at room temperature by mixing KMnO_4 (0.25 M) with fumaric acid (Fluka reagents). Reduction of Mn(VII) is followed by visual detection as follows: 2 ml of an aqueous solution of NaCl (1 M) are added to 1 ml of the sol taken before gelation occurs. This leads to the flocculation of MnO_2 . Complete reduction of Mn(VII) is obtained when the purple coloration cannot be seen anymore in the supernatant solution. A molar ratio $\rho = \text{KMnO}_4/\text{C}_4\text{H}_4\text{O}_4 = 3$ was used in order to get a mean oxidation state of manganese $Z = 4$ in the gel.

The role of the counter ion A was studied by using different AMnO_4 precursors. Therefore a proton exchange resin of Dowex type is first neutralized by an aqueous solution of LiOH, NaOH, NH_4OH , or $\text{N(CH}_3)_4\text{OH}$. Potassium permanganate is then eluted through the resin in order to

form the corresponding AMnO_4 (0.25 M) aqueous solution.

Reduction is performed with fumaric acid using a molar ratio $\rho = 3$. In all cases this leads to the formation of a dark brown transparent gel. This gel is spread onto a glass plate and dried in air at room temperature giving a black amorphous powder called xerogel. Calcination is then performed, up to 900°C . This leads to the formation of crystalline phases such as NaMnO_2 , LiMnO_2 , or KMnO_2 . These mixed oxides are then transformed into MnO_2 by ion exchange reactions according to the method already described in the literature (8–10). It consists of sulfuric acid treatment of the ternary oxide. The resulting powder is then filtered and dried in air at 90°C .

X-ray diffraction experiments were performed with a Philips diffractometer using the $\text{CuK}\alpha$ radiation. Thermal analysis measurements were performed in air at heating rates of $10^\circ\text{C} \cdot \text{min}^{-1}$ using a Netzsch STA 409 analyzer with the simultaneous recording of weight losses (TGA) and temperature variations (DTA). The mean oxidation state "Z" of manganese was determined via chemical titration by ferrous sulfate (11) with an accuracy of ± 0.02 . Infra-red spectra were recorded on a Perkin-Elmer 783 spectrophotometer by grinding the xerogel powder into KBr pellets.

Results

Reduction of AMnO_4 ($A = \text{Li, Na, K, NH}_4, \text{N(CH}_3)_4$) by fumaric acid at a pH between 7.5 and 8 is a fast and weakly exothermic reaction. It leads to the formation of transparent dark brown sols or gels depending on manganese concentration "C". A sol-gel transition is observed around $C = 0.1 M$. Just before gelation, the pH rises up to 9. After gelation, syneresis occurs at various times, between 20 min to 96 hr, depending on the chemical nature of the counter ion.

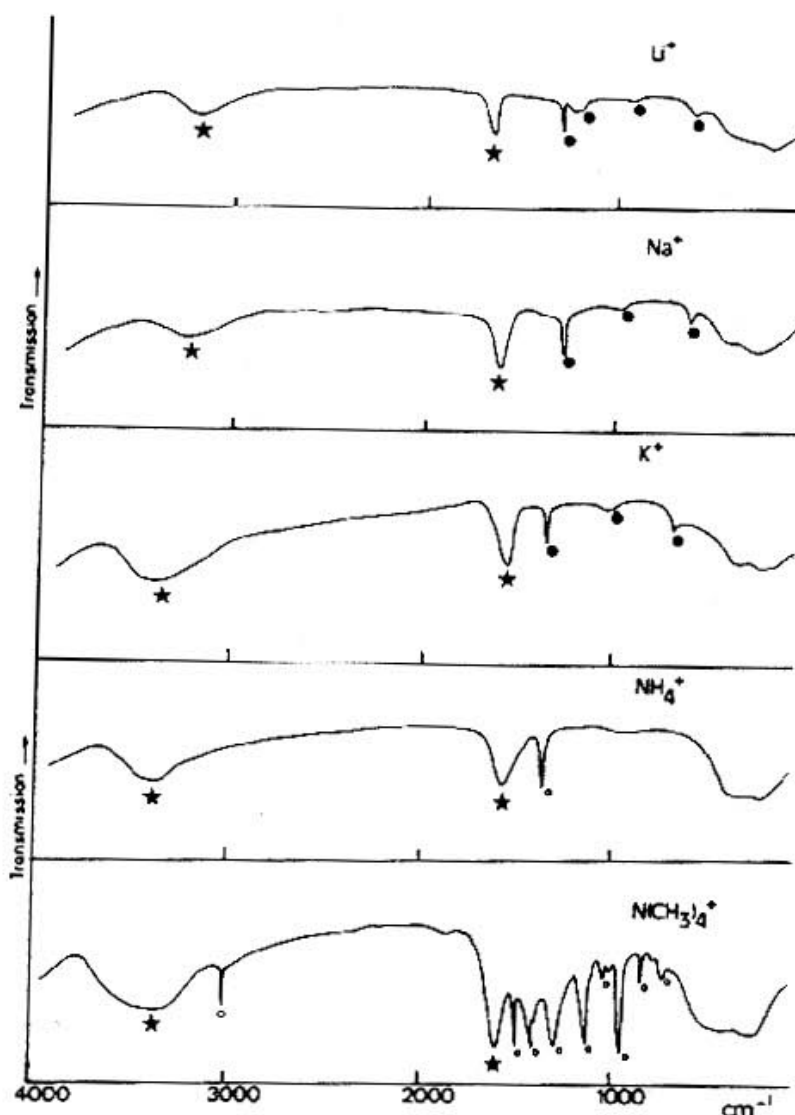


FIG. 1. IR spectra of the five xerogels ($A = \text{Li}, \text{Na}, \text{K}, \text{NH}_4, \text{N}(\text{CH}_3)_4$). ●, oxalate bands; ○, ammonia and $\text{N}(\text{CH}_3)_4$ bands; ★, H_2O and OH bands.

For all gels, the measured oxidation state Z of manganese is close to 4.

Infrared spectra of the xerogels (Fig. 1) exhibit bands typical of H_2O and OH species, as well as oxalate ions with three characteristic bands at 1330, 1060, and 780 cm^{-1} . Additional bands due to the presence of ammonium or tetramethylammonium ions can also be seen in the last two xerogels.

Lithium Permanganate Precursor

Thermal analysis (TGA and DTA) of the xerogel is shown in Fig. 2a. A total weight loss of about 40% is observed. The first two

endothermic peaks (94 and 166°C), the exothermic peak (300°C), and the broad endothermic peak around 370°C correspond to four different weight losses. They are probably due to the departure of water molecules and the thermal decomposition of oxalates. A small and continuous weight loss is then observed between 480 and 900°C while the crystallization of the spinel phase LiMn_2O_4 occurs, in agreement with the X-ray diffraction pattern performed at 600°C (Fig. 3a), and with the experimental oxidation state of manganese $Z = 3.45$. Finally a narrow endothermic peak and an abrupt weight loss (2.2%) at 940°C correspond to the formation

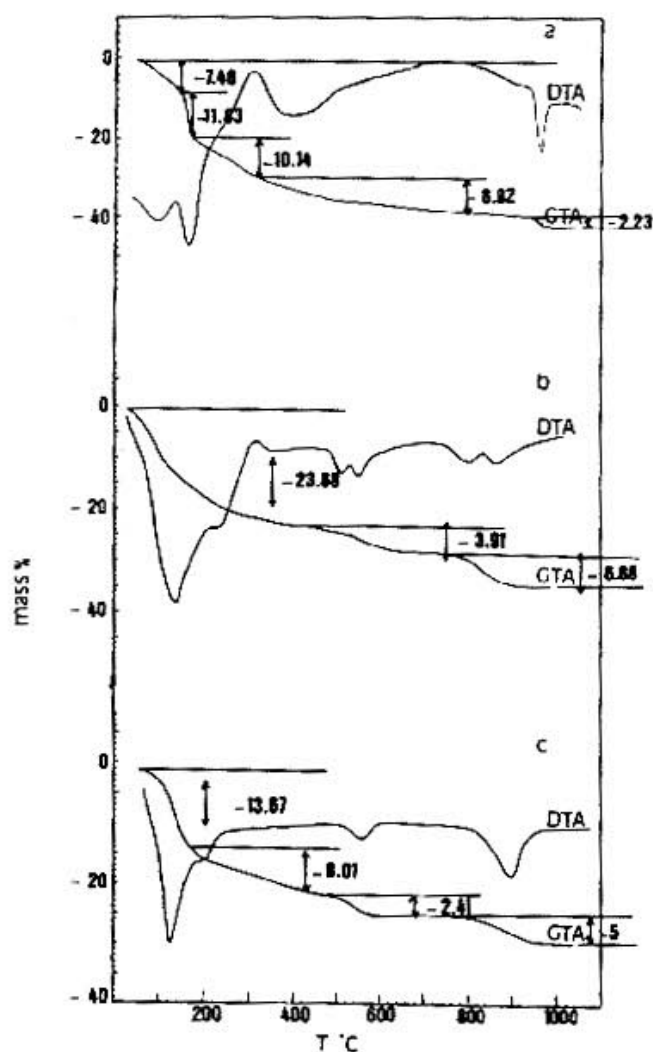
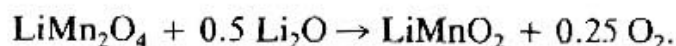


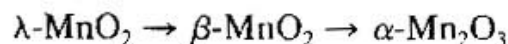
FIG. 2. Simultaneous thermal analysis (TGA and DTA) of the Li/Mn (a), Na/Mn (b), and K/Mn (c) xerogels.

of crystalline LiMnO_2 (Fig. 3b), with an experimental oxidation state of Mn, $Z = 3.12$, according to the following reaction:



Sulfuric acid treatment (2.5 M) during 2–5 hr of LiMn_2O_4 or LiMnO_2 lead to formation of a manganese dioxide, $\lambda\text{-MnO}_2$, as shown by X-ray diffraction (Fig. 3c). This compound has a defect spinel structure derived from the spinel structure of LiMn_2O_4 . A model was proposed in order to explain the effect of the acid treatment (8, 10). Both Li_2O and MnO appear to be removed from the solid network. Disproportionation of 2 Mn(III) into Mn(II) and Mn(IV) is supposed

to occur. Only Mn(II) species are soluble in the acid aqueous solution so that manganese in the resulting oxide exhibits a mean oxidation state close to $Z = 4$. DTA of this manganese dioxide agrees with this model. It shows two endothermic phenomena at 280 and 515°C which may be associated with the following phase transitions:



Sodium Permanganate Precursor

A black xerogel is obtained that remains amorphous below 400°C. Simultaneous thermal analysis of the xerogel (with a total weight loss of about 34% on GTA curve) is shown in Fig. 2b. Two endothermic phenomena at 135 and 200°C, and a broad peak at 345°C are visible. They are correlated to

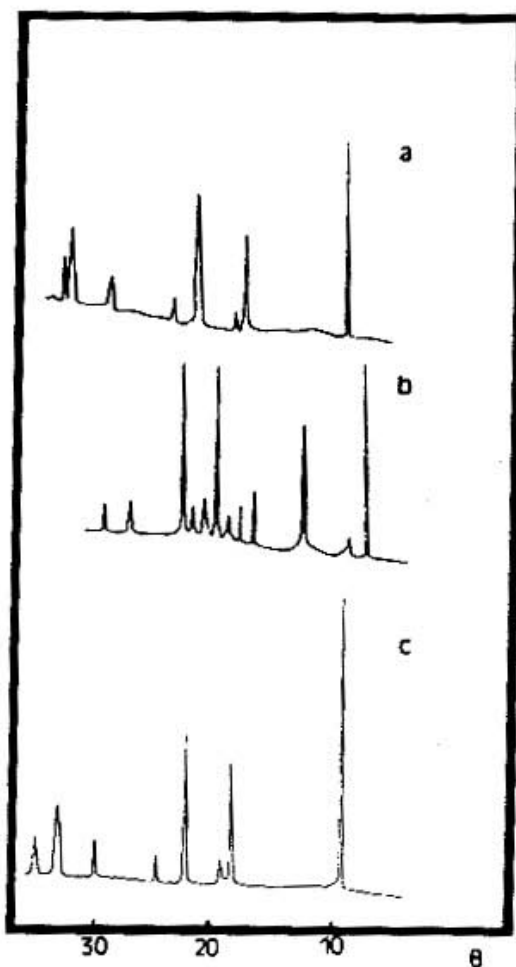


FIG. 3. X-ray diagrams of LiMn_2O_4 (a, 600°C/3 hr), LiMnO_2 (b, 1000°C/3 hr), and $\lambda\text{-MnO}_2$ (c, washed acid).

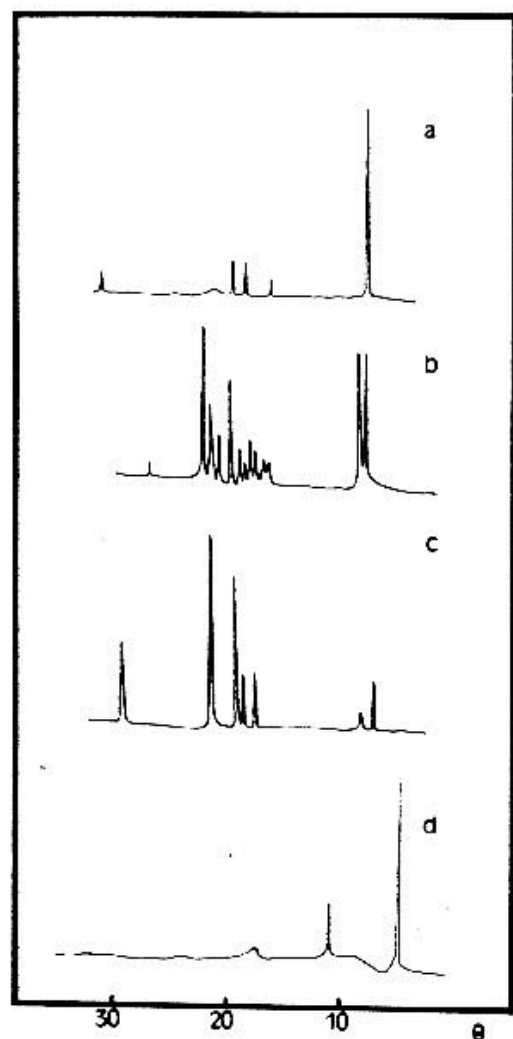


FIG. 4. X-ray diagrams of $\text{Na}_{0.7}\text{MnO}_2$ (a, 600°C/2 hr), $\alpha\text{-NaMnO}_2$ (b, 800°C/2 hr), $\beta\text{-NaMnO}_2$ (c, 1100°C/4 hr), and $\delta\text{-MnO}_2$ (d, washed acid).

a continuous weight loss (24%) up to 420°C and should correspond, as for the previous case, to the departure of water molecules and the decomposition of oxalates. A double endothermic peak and more weight loss (4%) occur between 420 and 660°C. They lead to the formation of the crystalline layered compound $\text{Na}_{0.7}\text{MnO}_2$ in agreement with the X-ray diffraction pattern at 600°C (Fig. 4a) and the measured oxidation state of Mn ($Z = 3.3$). A similar thermal behavior is again observed around 800°C together with the formation of $\alpha\text{-NaMnO}_2$ (oxidation state of manganese $Z = 3.1$), which leads to $\beta\text{-NaMnO}_2$ above 1000°C, as shown by X-ray diffraction (Fig. 4b).

Sulfuric acid treatment of $\text{Na}_{0.7}\text{MnO}_2$, $\alpha\text{-NaMnO}_2$, and $\beta\text{-NaMnO}_2$ leads as Clearfield and co-workers (12) mentioned to the formation of the $\delta\text{-MnO}_2$ polymorph of manganese oxide (Fig. 4d), with a measured oxidation state $Z = 3.84$. The X-ray diffraction pattern of this compound is given by Giovannoli *et al.* (13) who described it as a lamellar phase. But, only two diffraction peaks appear, with the following d -spacing: 7.24 and 3.62 Å, showing an important preferred orientation. DTA diagram of this compound shows two endothermic phenomena at 108 and 535°C which may be associated to the $\delta\text{-MnO}_2 \rightarrow \beta\text{-MnO}_2$ and $\beta\text{-MnO}_2 \rightarrow \alpha\text{-Mn}_2\text{O}_3$ transformations, respectively, as revealed by X-ray diffraction.

Potassium Permanganate Precursor

The black xerogel powder remains amorphous up to 500°C. As for the previous cases two endothermic phenomena are observed at low temperature (133 and 220°C). They must be related to the departure of water molecules and the decomposition of oxalates. The following exo- and endothermic peaks cannot be seen on the DTA curve despite the fact that a continuous weight loss still goes on. Two endothermic peaks with the corresponding weight losses (2.4 and 5.4%) are then seen around 480 and 900°C, respectively. X-ray diffraction does

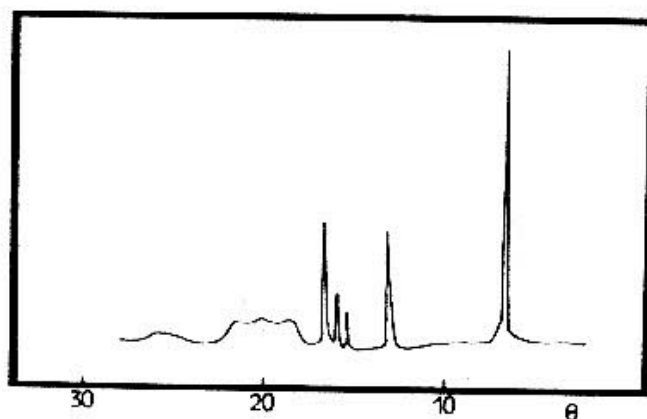


FIG. 5. X-ray diagram of KMnO_2 (600°C/3 hr).

not show any intermediate crystalline compound before the formation of the lamellar compound KMnO_2 around 600°C (Fig. 5), in agreement with the measured oxidation state of Mn, $Z = 2.96$. Therefore the attribution of the endothermic weight loss around 480°C is not obvious. According to the thermal analysis the sample cannot be completely transformed into KMnO_2 above 600°C as weight losses are still observed above 700°C . It seems that only one-third of the product is transformed into KMnO_2 around 600°C .

Sulfuric acid treatment of the KMnO_2 powder leads, after removing of K^+ and Mn^{2+} , to $\delta\text{-MnO}_2$ phase as with sodium compounds.

Ammonium Permanganate Precursor

The xerogel remains amorphous up to 500°C . Beyond this temperature it transforms directly into crystalline $\alpha\text{-Mn}_2\text{O}_3$. Infrared spectrum (Fig. 1) of the room temperature dried xerogel exhibits a strong absorption band around 1400 cm^{-1} , typical of (NH_4) species. At this stage, the measured oxidation state is $Z = 3.88$, a value close to $Z = 4$. The intensity of the band at 1400 cm^{-1} decreases together with the mean oxidation state ($Z = 3.66$) when the xerogel is dried at 90°C . The ammonium band even completely disappears after heating the sample for 5 hr at 300°C and the mean oxidation state becomes close to 3 ($Z = 3.16$). This suggests that ammonium ions act as reducing species toward manganese Mn(IV). Thermal analysis curves (Fig. 6a) show three endothermic phenomena with the related weight losses up to 400°C . A sharp exothermic peak is observed at 500°C . It corresponds to a small weight loss of 3.8% and leads to the crystallization of $\alpha\text{-Mn}_2\text{O}_3$.

Tetramethylammonium Permanganate Precursor

The xerogel is amorphous at room temperature and crystallizes into $\gamma\text{-Mn}_2\text{O}_3$

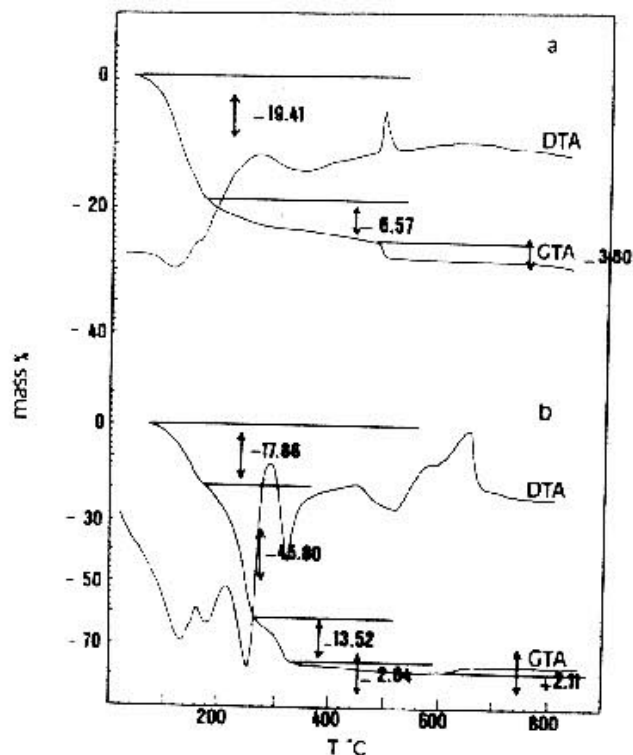


FIG. 6. Simultaneous thermal analysis (TGA and DTA) of the ammonium (a) and tetramethylammonium (b) xerogels.

around 350°C (Fig. 7a). Calcination of this compound above 550°C leads to the $\alpha\text{-Mn}_2\text{O}_3$ phase as in the previous case with ammonium counter ions (Fig. 7b). $\text{N}(\text{CH}_3)_4^+$ ions can be detected in the xerogel by infrared spectroscopy up to 350°C . Beyond this temperature they appear to be completely

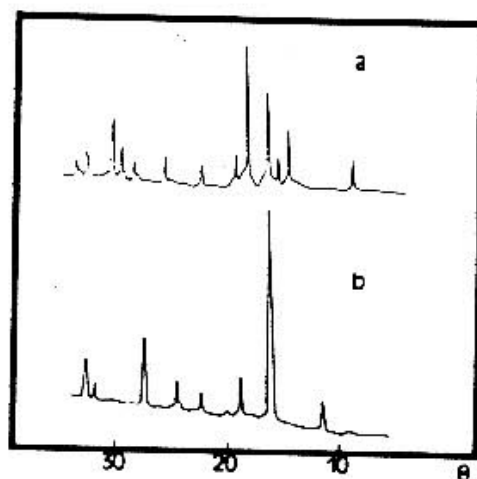


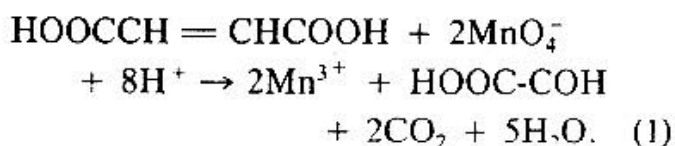
FIG. 7. X-ray diagrams of $\gamma\text{-Mn}_2\text{O}_3$ (a, $350^\circ\text{C}/5\text{ hr}$) and $\alpha\text{-Mn}_2\text{O}_3$ (b, $700^\circ\text{C}/3\text{ hr}$).

removed. Simultaneous thermal analysis (Fig. 6b) of the xerogel (with a total weight loss of 80% on GT curve) shows four endothermic peaks up to 400°C, with three successive weight losses. Several thermal effects with small weight variations are then observed between 500 and 660°C. Such a thermal behavior suggests a rather complex decomposition process. $N(CH_3)_4^+$ ions are presumably decomposed between 160 and 270°C into ammonia which then reduces MnO_2 into γ - Mn_2O_3 around 300°C. The endothermic phenomenon at 324°C could correspond to the crystallization of γ - Mn_2O_3 , which then leads to α - Mn_2O_3 around 500°C. The combustion of residual carbon species can be responsible for the exothermic peak and the weight increase at 600°C.

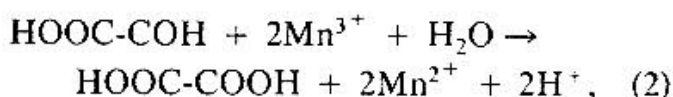
Discussion

Stable manganese oxide gels can be easily obtained via the reduction of permanganate $AMnO_4$ aqueous solutions with fumaric acid. According to literature, such a reduction does not lead directly to Mn(IV). Depending on the experimental conditions, Mn(II) and Mn(III) species are formed.

These results can be explained by reference to the known mechanism of oxidation of fumaric acid by MnO_4^- (14, 15). Around $pH = 4$, Mn^{3+} and glyoxylic acid are formed according to



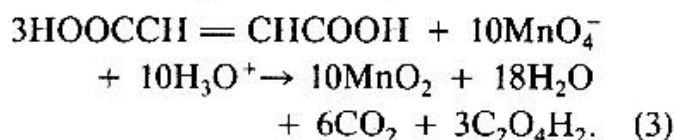
Under basic conditions ($pH > 7$), the carbon-carbon bond cannot be cleaved, but the aldehyde function could be oxidized according to



leading to oxalic acid formation. Under these conditions, Mn^{2+} ions are not stable

and could be oxidized into Mn_2O_3 or MnO_2 , with an excess of Mn(VII). This is experimentally obtained with a molar ratio $(KMnO_4)/(C_4H_4O_4) = 3$. Chemical titration then shows that the mean oxidation state of manganese is $Z = 4$.

Following this hypothesis, the optimum stoichiometry would be $\rho = 10/3 = 3$:



This mechanism shows that the MnO_2 gels contain adsorbed oxalate and hydroxyl ions in agreement with IR spectra.

Metal cations are hydrolyzed in the presence of water giving rise to more or less hydroxylated solute species. Hydroxylation depends mainly on the positive charge of the cation and the pH of the aqueous solution. In our experimental conditions, at a pH close to 7, Mn(VII) ions are surrounded by four oxygen atoms giving the well-known permanganate ion $(MnO_4)^-$. Hydroxylation is favored when the oxidation state of manganese decreases so that Mn(IV) species are hydroxylated. Condensation then occurs via olation and oxolation. Gelation arises from the formation of an hydrous manganese oxide network. Counter cations A^+ are not hydroxylated under our experimental conditions. They are only solvated by dipolar water molecules. They are therefore not able to give rise to condensed species and remain trapped inside the gel network.

Manganese oxide gels lead to amorphous xerogels upon drying at room temperature. However their thermal behavior as well as the crystalline phases obtained upon heating depend on the nature of the counter cation A. Alkaline cations (Li^+ , Na^+ , K^+) react in the solid state with the manganese oxide leading to the formation of mixed oxide phases. In all cases, trivalent manganese $AMnO_2$ compounds are obtained at high temperature. However different crys-

talline phases such as LiMn_2O_4 or $\text{Na}_{0.7}\text{MnO}_2$ can be formed during the thermal treatment. They suggest that some solid state reactions first occur in the amorphous phase in which only part of the alkali ions are involved. This could be due to the formation of oxalates or carbonates that are known to react slowly in the solid state. According to the literature, such mixed oxides can also be obtained via the solid state reaction of MnO_2 or Mn_2O_3 with alkali carbonates (16–18).

Ammonium and tetramethylammonium cations are dissociated upon heating. They lead to the trivalent manganese oxide $\alpha\text{-Mn}_2\text{O}_3$ around 500°C. Until now, such Mn_2O_3 phases were obtained by adding ammonia to aqueous solutions of MnSO_4 in the presence of hydrogen peroxide, or upon vacuum reduction of $\gamma\text{-MnO}_2$ at 500°C (19).

Mixed oxides AMnO_2 can be transformed into manganese dioxide MnO_2 upon oxidation in a sulfuric acid solution. Experiments show that A^+ and Mn^{2+} ions are released into the solution while the solid network progressively transforms into MnO_2 . The nature of the obtained crystallographic forms of MnO_2 depends on the different alkali precursors. It is well known that an acid treatment at room temperature cannot induce important structural transformations. Only topochemical reactions are expected and thus the different forms of MnO_2 will have to be structural relationships with the mixed oxides AMnO_2 derived from the molecular precursors AMnO_4 :

—a defect-spinel type for $\lambda\text{-MnO}_2$ which is obtained from the lithiated manganites LiMn_2O_4 and LiMnO_2 . These compounds belong both to the spinel-series $\text{Li}_{1+x}\text{Mn}_2\text{O}_4$ ($0 < x < 1$) evidenced by electrochemical insertion of lithium in LiMn_2O_4 (10, 20). However, it seems that it is difficult to obtain by acid treatment all the compounds of the $\text{Li}_{1+x}\text{Mn}_2\text{O}_4$ series, since a moderate acid treatment (at pH = 2 during 30 min) of

$\text{Li}_2\text{Mn}_2\text{O}_4$ leads only to a mixing of LiMn_2O_4 and $\lambda\text{-MnO}_2$.

—a lamellar character for $\delta\text{-MnO}_2$ which is obtained from the manganites containing sodium and potassium: $\alpha\text{-NaMnO}_2$, $\beta\text{-NaMnO}_2$, $\text{Na}_{0.7}\text{MnO}_2$, KMnO_2 . The sodium compounds, which have sodium contents close to that of manganese, are effectively characterized by the existence of edge-linked manganese oxygen octahedra, which give rise to tridimensional layers (16). The potassium compound KMnO_2 has a layer structure of the same type than sodium compounds. Then it is not surprising to obtain in all cases the $\delta\text{-MnO}_2$ lamellar structure. As for the previous case, a moderate acid treatment (at pH = 6 during 30 min) of the compounds $\alpha\text{-NaMnO}_2$ and $\beta\text{-NaMnO}_2$ lead to a mixture of $\text{Na}_{0.7}\text{MnO}_2$ and $\delta\text{-MnO}_2$; under the same conditions, KMnO_2 gives rise to an intermediate composition $\text{K}_{0.5}\text{MnO}_2$.

Acknowledgment

Financial support by the Direction des Recherches Etudes et Techniques (DRET) is gratefully acknowledged.

References

1. F. W. DAMPIER, *J. Electrochem. Soc.* **121**, 656 (1974).
2. M. BELTOWSKA-BRZEZINSKA, E. DUTKIEWICZ, AND J. STUCZYNISKA, *J. Electroanal. Chem.* **135**, 103 (1982).
3. G. PISTOIA, *J. Electrochem. Soc.* **129**, 1861 (1982).
4. J. C. NARDI, *J. Electrochem. Soc.* **132**, 1787 (1985).
5. J. LIVAGE, M. HENRY, AND C. SANCHEZ, *Prog. Solid State Chem.* **18**, 259 (1988).
6. L. ZNAIDI, N. BAFFIER, J. P. PEREIRA-RAMOS, AND R. MESSINA, *Solid State Ionics* **28–30**, 886 (1988).
7. L. ZNAIDI, N. BAFFIER, AND M. HUBER, *Mater. Res. Bull.* **12**, 1501 (1989).
8. J. C. HUNTER, *J. Solid State Chem.* **39**, 142 (1981).
9. D. TANG, D. A. JEFFERSON, I. J. PICKERING, A. HARRIMAN, J. M. THOMAS, AND R. D. BRYDSON, *J. Solid State Chem.* **79**, 112 (1989).
10. J. B. GOODENOUGH, M. M. THACKERAY, W. I. F. DAVID, AND P. G. BRUCE, *Rev. Chim. Miner.* **21**, 435 (1984).

11. M. J. KATZ, R. C. CLARKE, AND W. F. NYE, *Anal. Chem.* **28**, 507 (1956).
12. X-M. SHEN AND A. CLEARFIELD, *J. Solid State Chem.* **64**, 270 (1986).
13. R. GIOVANOLI, E. STHÄHLI, AND W. FEIKNECHT, *Helv. Chim. Acta* **53**, 454 (1970).
14. M. JAKY, L. I. SIMANDI, L. MAVOS, AND I. MOLNAR-PERL, *J. Chem. Soc. Perkin Trans 2*, 1565 (1973).
15. L. I. SIMANDI AND M. JAKY, *J. Chem. Soc. Perkin Trans. 2*, 1856 (1973).
16. J. P. PARANT, R. OLAZCUAYA, M. DEVALETTE, C. FOUASSIER, AND P. HAGENMULLER, *J. Solid State Chem.* **3**, 1 (1971).
17. M. A. LEHMANN AND K. TESKE, *Z. Anorg. Allg. Chem.* **336**, 197 (1965).
18. S. HIRANO, R. NARITA, AND S. NAKA, *Mater. Res. Bull.* **19**, 1229 (1984).
19. T. E. MOORE, M. ELLIS, AND P. W. SELWOOD, *J. Amer. Chem. Soc.* **72**, 856 (1950).
20. M. M. THACKERAY, W. I. F. DAVID, P. G. BRUCE, AND J. B. GOODENOUGH, *Mater. Res. Bull.* **18**, 461 (1983).